ELSEVIER

Journal of Structural Geology 30 (2008) 701–709

JOURNAL OF STRUCTURAL GEOLOGY

www.elsevier.com/locate/jsg

Quantifying fault breccia geometry: Dent Fault, NW England

K. Mort, N.H. Woodcock*

Department of Earth Sciences, University of Cambridge, Downing Street, Cambridge CB2 3EQ, UK

Received 29 July 2007; received in revised form 12 February 2008; accepted 14 February 2008
Available online 21 February 2008

Abstract

A geometric classification of fault breccia borrowed from the cave-collapse literature has been suggested as an alternative to available genetic classifications. Here, image analysis is used to explore geometric discrimination between the visually assigned classes of crackle breccia, mosaic breccia and chaotic breccia, using samples from the well-understood Dent Fault, northwest England. Clast sphericity and surface roughness show some correlation with the breccia classes, but particle size distributions and their fractal dimension show none. A more useful parameter is the percentage of sample area occupied by clasts. Crackle breccia has >75% clasts, mosaic breccia 60–75% clasts, and chaotic breccia has <60% clasts. The eye is also good at judging the tessellation (goodness-of-fit) of clasts, and a semi-quantitative approach to assessing this parameter is explored. The average degree of rotational misfit of the clasts is strongly related to breccia class: crackle breccia involves less than 10° average rotation, mosaic breccia 10–20° and chaotic breccia more than 20° rotation. Comparison charts are provided for semi-quantitative classification of fault breccias.

Keywords: Fault rock; Crackle breccia; Mosaic breccia; Chaotic breccia

1. Introduction

Vigorous debates over fault rock classification have centred on the distinction of the mylonite series from the cataclasite series, and on the subdivision and genesis of these rocks (see review by Snoke et al., 1998). Relatively little attention has been given to the classification of fault breccias, despite their evident importance in the upper crust. Genetic classifications are available, but an easily applied non-genetic scheme has yet to find acceptance. One promising approach (e.g. Laznicka, 1988; Koša et al., 2003; Woodcock et al., 2006) has been to borrow terms in common use in the cave-collapse literature (e.g. Loucks, 1999). These terms – crackle breccia, mosaic breccia and chaotic breccia – qualitatively describe the increasing degree of disaggregation of initially intact rock. Importantly, they can be used whether the breccia clasts are separated by fine-grained matrix or crystalline cement (Woodcock et al., 2006); a factor too little stressed in existing classifications.

The aim of the present study is to explore the possibility of quantifying the crackle–mosaic–chaotic breccia spectrum, at least to the point where a semi-quantitative comparison chart might be produced for the field geologist. This quantification has been attempted with image analysis software, using examples of breccias and coarse cataclasites ('microbreccias') from the Dent Fault, NW England. Some problems of measuring such parameters as clast roundness, surface roughness, clast percentage of sample area, particle size distributions will be discussed. The eye is also adept at judging the goodness-of-fit of clasts, and a possible route to quantification of this geometrical parameter is described. The results of the Dent Fault study are then used to create comparison charts for use in the field or laboratory.

2. Fault breccia classification

2.1. Distinction from other fault rocks

The influential classification of fault rocks by Sibson (1977) characterised fault breccia as coarse rock (at least 30% visible clasts) that lacked cohesion at the time of faulting. However,

* Corresponding author. Fax: +44 1223 333450.
E-mail address: nhw1@esc.cam.ac.uk (N.H. Woodcock).

0191-8141/$ - see front matter © 2008 Elsevier Ltd. All rights reserved.
doi:10.1016/j.jsg.2008.02.005

Sibson, following Spry (1969) and Higgins (1971), recognised that some coarse fault rocks may have retained cohesion during their formation, and termed these rocks 'crush breccia'. The unstated implication of the distinction between crush breccia and fault breccia was that crush breccias have a fine-grained matrix produced by fragmentation during faulting, whereas fault breccias have post-faulting crystalline cement. Killick (2003) suggested subsuming crush breccias in the cataclasite or mylonite series, but did not address the matrix/cement issue. Woodcock and Mort (in press) pointed out the difficulty in distinguishing matrix from cement, and in assessing primary cohesion, in the field, and suggested that all coarse fault rocks (30% of clasts larger than 2 mm) should be termed breccia, irrespective of their primary or present state of cohesion. The 2 mm limit is in harmony with sedimentological usage and with an earlier suggestion by Laznicka (1988). Matrix is defined by Woodcock and Mort (in press) as fine-grained particulate material – how fine is discussed by them – whether produced by local fragmentation of larger particles or by later introduction of more exotic sediment. Cement is defined as crystalline material grown in place, either as infill of void space or as a replacement of clasts or matrix. The term infill (Taylor, 1992) can be applied to any post-faulting void-filling cement or matrix.

2.2. Classification of fault breccias

The most common classifications of fault breccia are genetic, and aim to discriminate cataclastic mechanisms. For instance, Sibson (1986) recognised implosion breccias, attrition breccias and crush breccias as formed at dilational, neutral and antidilational sites along faults, respectively. However, his recognition criteria – matrix composition, clast composition, clast size distribution, internal clast deformation and texture – are all objectively observable. More ambitiously, Jébrak (1997) distinguished eight different brecciation mechanisms, imperfectly characterised by a combination of clast roughness, fabric, dilation ratio, and the fractal dimension of the particle size distribution. Particle size distributions have also been widely used, though mostly on cataclasites rather than breccias, in attempts to correlate fractal dimension with a cataclastic mechanism (e.g. Sammis and Biegel, 1989; Blenkinsop, 1991).

Most non-genetic classifications of fault breccias only subdivide them on the basis of their primary cohesion (e.g. Sibson, 1977) or their clast size (e.g. Spry, 1969). Laznicka (1988) proposed a more comprehensive descriptive scheme for breccias in general, but its complexity means that it has not been much used. The scheme does, however, use the textural distinction between crackle, mosaic and chaotic (or 'rubble') breccia. This distinction has been used successfully by Koša et al. (2003) for breccias formed along syndepositional faults in limestones. However, these authors restrict the terms crackle and mosaic to breccias formed by gravitational collapse into voids, and substitute the terms tight and loose for those formed directly by faulting. Given the difficulty of assigning a formation mechanism to a specific breccia (Koša et al., 2003), Woodcock et al. (2006) have advocated the use of the terms crackle, mosaic and chaotic for all fault-related breccias, irrespective of origin. This is the textural spectrum addressed in the present study.

3. Image analysis methodology

3.1. Sample preparation and measurement

Sixteen hand specimen samples were chosen from collections made along the Dent fault zone, NW England. In the sampled area, this steep reverse-oblique fault zone throws Lower Carboniferous limestones against Ordovician and Silurian mudstones. The regional setting and local context of these fault rocks have been described by Woodcock and Rickards (2003), Tarasewicz et al. (2005), Woodcock et al. (2006) and Woodcock et al. (in press). The breccias formed by dilational fragmentation in fault damage zones rather than attrition in fault cores, and some may have involved collapse into transient or persistent fault voids. The samples are mostly of limestone (seven samples) or dolomitised limestone (four), with the remainder being of mudstone (four) or sandstone (one), all with carbonate cements. They were chosen to span the spectrum of textures from crackle to mosaic breccia (Fig. 1) and classified qualitatively by eye at hand specimen scale.

Breccia textures were digitally scanned or photographed from thin sections (eight samples, see caption to Fig. 1) or acetate peels, with carbonate lithologies stained to highlight compositional differences. The areas available for study varied from about 5 to 20 cm^2. The digital images were then traced on-screen in the CorelDraw graphics package to delineate clasts. The resolution used meant that clasts as small as about 0.02 mm could have been adequately measured. Most clasts analysed were in the range 0.2–10 mm, well above this observation threshold. Clasts both more than and less than 2 mm were included in the analysis, as the textures were common to all clasts. The traced images were analysed using the ImageJ software (Rasband, 1997–2006), although the sister program ScionImage (Scion Corporation, 2006) was additionally used to calculate a surface roughness coefficient, described below. In all, six separate parameters were measured, discussed in the following sections.

To determine the number of clasts needed to constrain the measured parameters, a typical sample, number 11, was digitised over a large enough area to yield 481 clasts. Three sub-sets of 120 clasts were randomly selected. Three parameters – area, roundness and roughness of clasts – were then measured from the three sub-sets for increasing sample sizes of 1–120 (Fig. 2). Parameter values stabilized in all tests between $n = 40$ and $n = 60$. A lower measurement limit of 60 clasts was therefore used in the present study.

3.2. Sphericity

The sedimentological definition of grain sphericity in three dimensions derives from Waddell (1933):

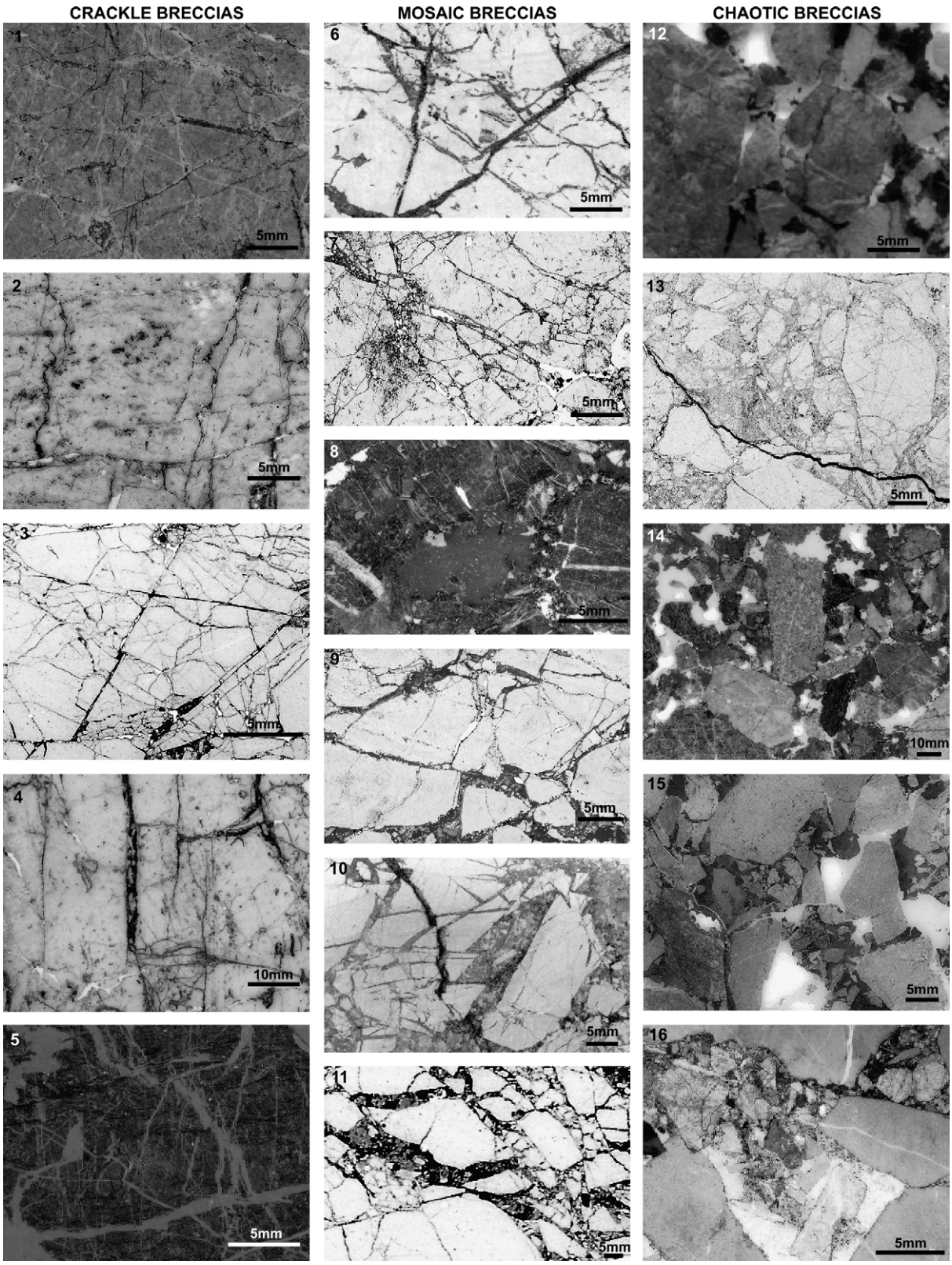

Fig. 1. The 16 thin sections (1, 2, 8, 12–16) and acetate peels used in the textural analysis, photographed in transmitted light. They are arranged in increasing order of textural development. One to five was visually assessed as crackle breccias, 6–11 as mosaic breccias and 12–16 as chaotic breccias. All samples were stained with combined alizarin red-S and potassium ferricyanide so that, in a monochrome image, dolomite or non-calcareous components generally appear light and calcite or ferroan calcite components appear darker.

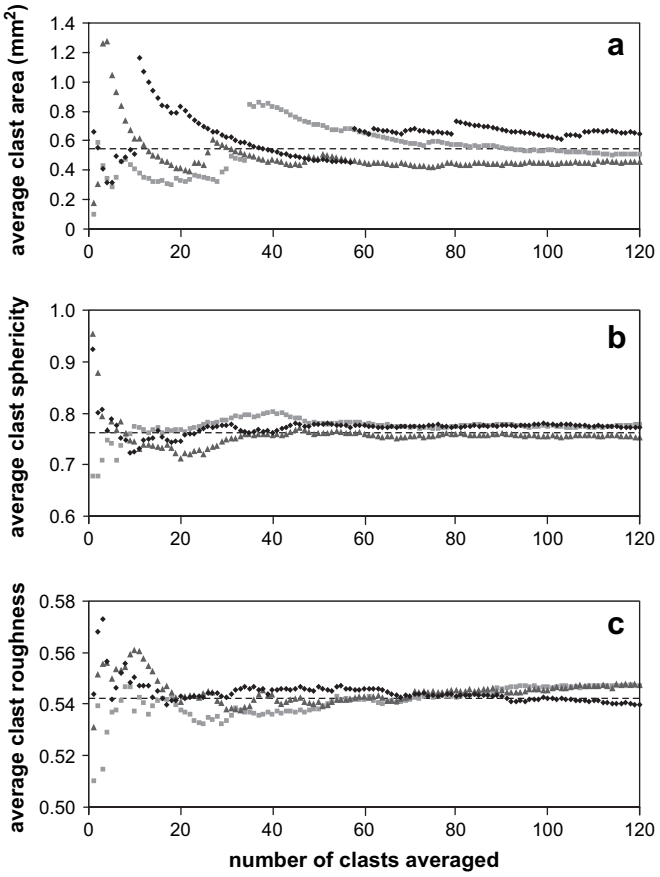

Fig. 2. Plots of three measured parameters against sample size for three subsamples of up to $n = 120$ clasts from sample 11 (with total $n = 481$). The dashed horizontal line is the mean value for the whole sample. See text for further explanation. Note the stabilization of parameter values by about $n = 60$.

$$S_w = \left(V_p/V_{cs}\right)^{1/3}$$

where V_p is the clast volume and V_{cs} is the volume of the smallest circumscribing sphere. The common 2D measure was suggested by Riley (1941):

$$S_R = \left(D_i/D_c\right)^{1/2}$$

where D_i and D_c are the diameters of the inscribed and circumscribing circles. ImageJ determines D_c but not D_i, making estimation of Riley's sphericity problematic. Instead, a 2D adaptation of Waddell's sphericity was used:

$$S_{W2} = \left(A_p/A_{cs}\right)^{1/2}$$

where A_p and A_{cs} are the areas of the clast and the circumscribing circle. A test using a natural sample breccia (Fig. 3) showed a strong correlation of this modified Waddell parameter against the Riley parameter, suggesting its suitability as a sphericity measure.

ImageJ calculated a value of circularity (S_c):

$$S_c = 4\pi\left(A_p/P^2\right)$$

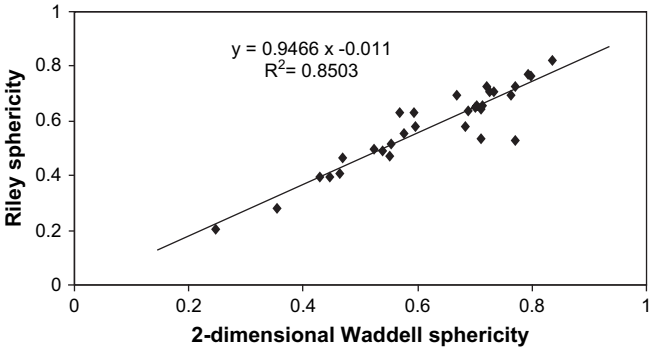

Fig. 3. Plot of Riley's sphericity parameter against the 2D adaptation of Waddell's parameter for 31 breccia clasts. Sample is not one of those in Fig. 1. See text for discussion.

where A_p is the area of the clast and P is the perimeter length of the clast. This measure is not considered as robust as the modified Waddell sphericity because, for complex objects, circularity is strongly dependent on the surface roughness of the clast, discussed separately below.

3.3. Surface roughness

Sedimentological literature (Folk, 1965) refers to the degree of surface irregularity of clasts as roundness, but here the more explicit term surface roughness is preferred. The commonly used comparison chart of Powers (1953) is based on Waddell's (1933) method of comparing the radii of curvature of all the grain asperities with that of its inscribed circle. A more practical method is to compare the length of the irregular grain boundary against the length of a smooth reference shape. In this study, an ellipse with the same area and axial ratio as the clast was chosen as a more general reference shape than a circle or rectangle. ImageJ finds the longest diameter of each clast, fits a bounding rectangle with one side parallel to this diameter, then assigns an ellipse axial ratio similar to that of this rectangle.

Clark and James (2003) used an alternative roughness measure derived from a macro within ScionImage that progressively thickens the outline of a clast by convolving the border with a kernel of increasing diameter. The total area of the border is then compared to the diameter of the kernel. The method was not used in the present study because it becomes unstable for small or elongate clasts, due to overlap of the thickening border.

3.4. Clast size, sorting and fractal dimension

The first two of these measures are straightforward output from ImageJ. The size of each clast is recorded as its maximum diameter. The degree of sorting is defined as the standard deviation of the linear dimensions of the clasts (Folk, 1965). A more sophisticated measure of the variation in clast size is obtained by plotting a log–log plot of clast diameter against the number of clasts greater than that diameter (Fig. 4). It has been well established. (e.g. Blenkinsop, 1991; Turcotte, 1992) that

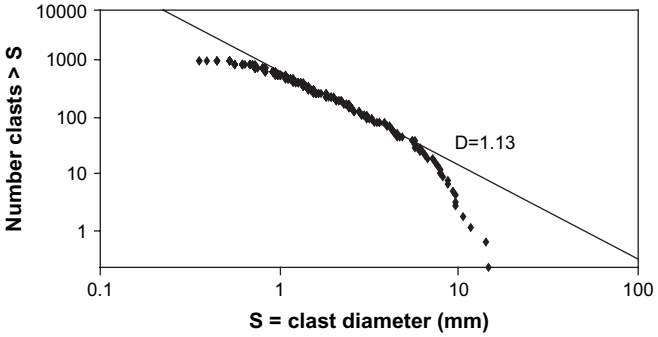

Fig. 4. Example of a log–log plot of clast size against the number of clasts greater than that size for sample 9. Fractal behaviour is indicated by the straight line between two fractal limits. The gradient of the line is the 2D fractal dimension for this sample.

a straight line pattern on this plot indicates a self-similar or fractal distribution of clast sizes, partly characterised by the gradient of the straight line: the fractal dimension. Fractal dimensions are reported below for the Dent Fault samples, but the robustness of these results is debatable. All samples show a fractal range of less than an order of magnitude and whilst the lower size limit does not seem to be an artefact of the measurement techniques, the upper size limit is strongly limited by the size of the studied samples.

3.5. Clast concentration

The area of clasts in the 2D surface was summed and expressed as a percentage of the total area of the sample, including also matrix, cement and open voids. For this measurement, clasts that overlap the edge of the field of view are ignored, and the total area taken along their inner boundaries (Coster and Chermant, 2001). Clast concentration is inversely proportional to the 2D dilation of the rock only if clast margins are neither fragmented, to produce fine-grained matrix, nor dissolved.

3.6. Tessellation

The human ability to characterise breccia texture is due partly to assessment of tessellation of clasts: their goodness-of-fit to one another in the manner of a jigsaw puzzle. Optimal packing software, designed to minimise wastage in manufacture of 2D pieces cut from sheet material, has addressed this problem, but only for simple shapes. There is an additional problem in 3D that clasts may have moved in and out of the plane of measurement during deformation.

In the absence of an automated approach, 10 out of the 16 samples in this study (1–2, 6–8, 14–16) were tessellated manually using the following procedure.

a) Clasts (between 60 and 400) were fitted back together by eye using the CorelDraw graphics package. The restriction was made that clasts could only fit to their nearest neighbours. The eye seems to use both *edge matching*, using similarity of clast boundaries, and *corner matching*, identifying corners on neighbouring clasts that add up to 360° (Fig. 5b).
b) The tessellated image was reanalysed by ImageJ, to find the new clast concentration. The higher this parameter, the better the fit. In all samples, a value of greater than 93% was achieved.
c) Each clast was identified on both the original and tessellated images and the relative angle of rotation of each clast was measured. The mean rotation angle for the sample

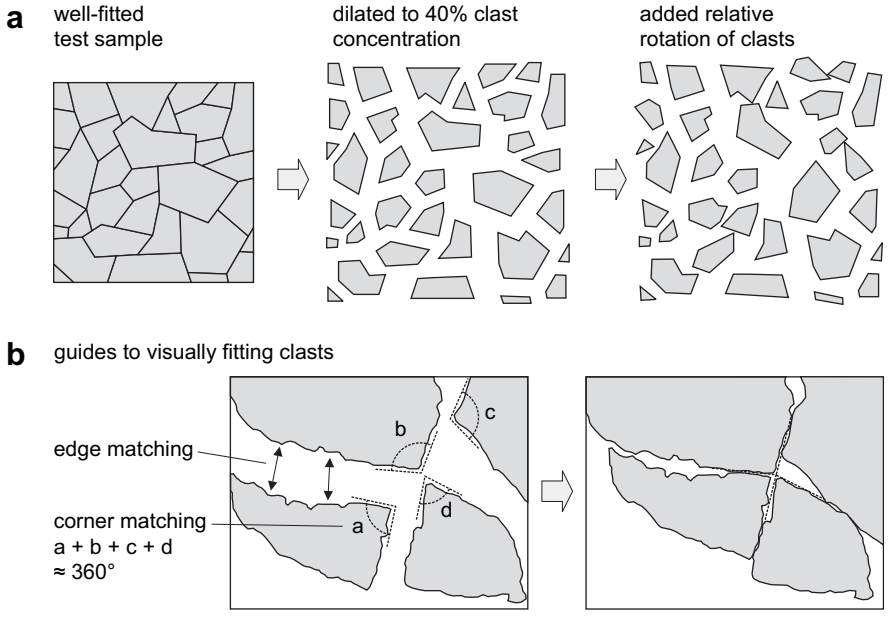

Fig. 5. Clast tessellation. (a) Test sample with clasts first dilated, then rotated. Goodness-of-fit is harder to judge in the sample with rotation. (b) The visual guides for fitting clasts by matching edges and corners. See text for discussion.

was calculated. This rotation angle seems to be important in the eye's assessment of goodness-of-fit (Fig. 5a).

This manual tessellation method is very time-consuming. Algorithms for automated tessellation of breccia clasts have been explored but not implemented, and are beyond the scope of this study.

4. Results of textural analysis

The results of the geometrical analysis of all 16 samples are shown in Fig. 6. All graphs show the samples by the degree of disaggregation of the texture as qualitatively assessed by eye. The continuous variation is divided into three classes – crackle, mosaic and chaotic – with the mean and standard deviation for each parameter shown for each class.

The sphericity of clasts is seen to increase (Fig. 6a) and the surface roughness to decrease (Fig. 6b) as the texture becomes more disaggregated. However, the ranges of sphericity and roughness are small and the differences between their means are not significant at the 95% confidence level. Nevertheless, rounding of clasts is a commonly predicted result of attrition in fault zones (e.g. Sibson, 1986). The small range of values in this study may reflect the probable formation of the Dent Fault breccias by implosion into transient dilational sites (Tarasewicz et al., 2005), or by collapse into more persistent fault voids (Woodcock et al., 2006). Only limited rounding by interclast collisions would be expected with these processes.

No visible trend between breccia classes can be seen in the sorting of particle size (Fig. 6c), or in the more sophisticated measure of the particle size distribution: the fractal dimension (Fig. 6d). The average 3D fractal dimension for all the Dent Fault samples is 2.68 ± 0.47, higher than would be expected for their dilational origin (Blenkinsop, 1991) and close to the theoretical value of 2.58 for attritional breccias (Sammis and Biegel, 1989). A detailed investigation of the fractal dimensions of the Dent Fault breccias is beyond the scope of this study. It would need to address the relatively limited range of fractal behaviour – less than an order of magnitude – and the grain-size breaks at around 1–3 mm in over half the samples, which might be due to some control by precursor lithology.

By contrast, there is a clearer correlation with breccia class of the clast concentration (Fig. 6e). The difference between the means for mosaic and chaotic breccias is significant at the 90% confidence level and that for crackle and mosaic breccias at the 95% level. This parameter therefore gives a convenient quantitative guide to distinguishing breccia classes, with suggested class bounds at 60% and 75% clast concentration.

The tessellation of clasts was measured in the two ways already described. The percentage area occupied by the visually refitted clasts is slightly higher for crackle breccias than for other classes, but showed no significant difference between mosaic and chaotic breccias (Fig. 6f). A better measure of tessellation is the average rotation of clasts needed to achieve a strong fit (Fig. 6g). Average angles of 5° for crackle breccia, 15° for mosaic breccia and 29° for chaotic breccia are all

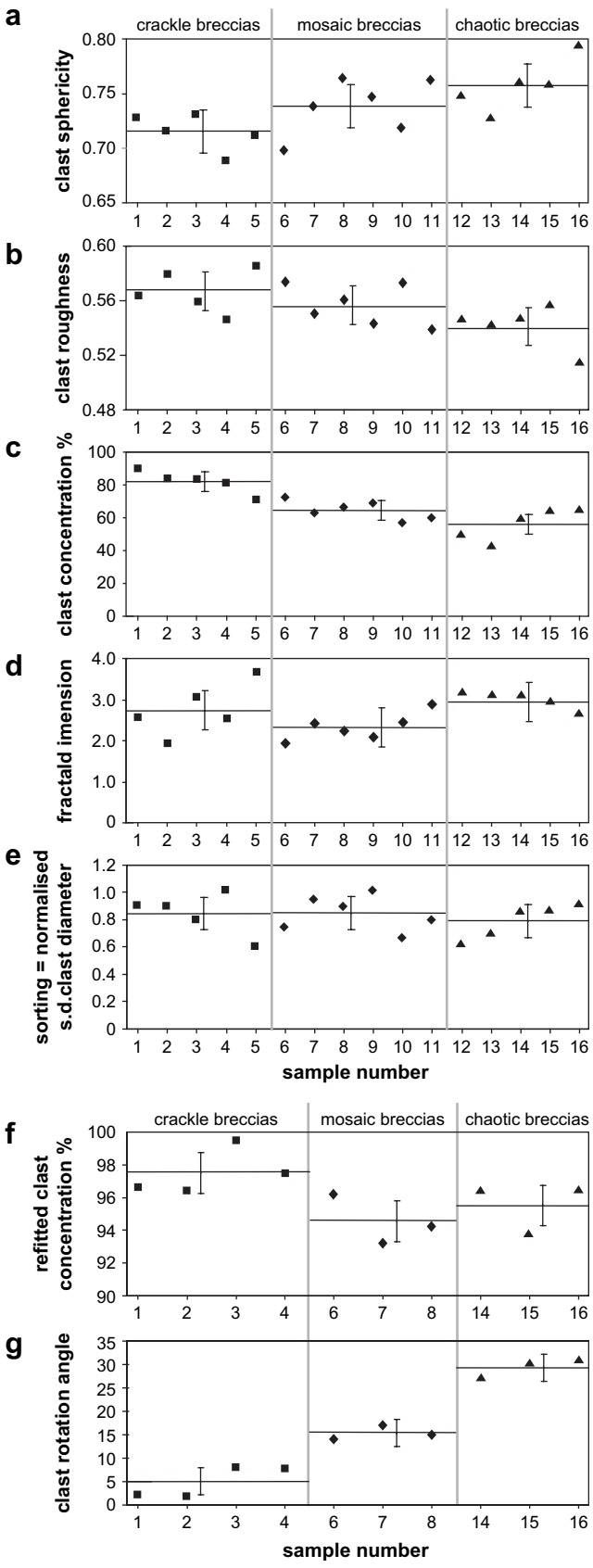

Fig. 6. Geometrical parameters for all (a–d) or some (e–f) of the breccia samples in Fig. 3. Samples are arranged in order of increasing disaggregation. Crackle, mosaic and chaotic breccias are separately ornamented, and mean parameter values and their standard deviations are shown for each class.

significantly different at the 95% level. Boundaries between classes are proposed at the rounded values of 10° and 20°.

5. Semi-quantitative fault breccia classification

The aim of this study has been not only to explore the quantification of fault breccia textures but also to use the results to help the field geologist classify fault breccias. The analysis has shown that, whilst there is some correlation of clast sphericity and roughness with the spectrum of crackle, mosaic and chaotic textures, the best discriminators are the clast concentration, and the rotation of clasts away from their fully fitted condition. These parameters are represented in Fig. 7a, b, respectively.

Five increments of percentage clast area are shown in Fig. 7a. Those at 75% and 60% clast concentration are important as the boundaries proposed here for the crackle, mosaic and chaotic breccia textures. Three increments of average clast rotation are shown (Fig. 7b) all drawn at 60% clast concentration. The 10° and 20° increments are the boundaries of the breccia classes proposed here. An even more realistic chart (Fig. 7c) shows increments of clast concentration and

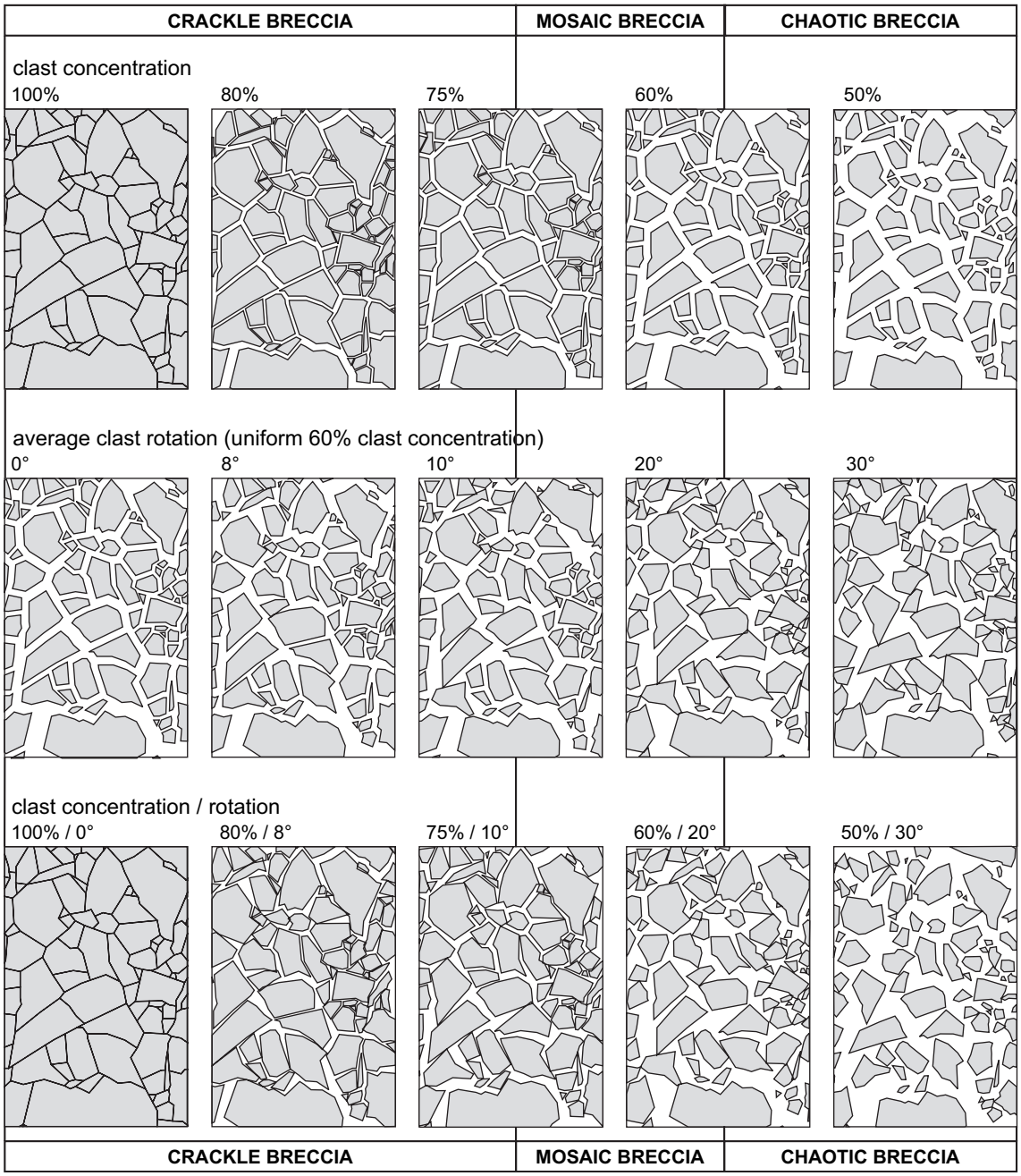

Fig. 7. A simplified crackle breccia progressively deformed (a) by decreasing the clast concentration, (b) by increasing the average rotation of clasts, at constant 60% clast concentration, and (c) by combining the effects of clast concentration and rotation. Version (c) provides a practical comparison chart for use in the field or lab.

rotation occurring together. This version provides a practical comparison chart for classifying natural breccia textures in the field.

The clast concentration limits to breccia classes can be displayed (Fig. 8) on a ternary diagram of fault breccias of the type proposed by Woodcock et al. (2006). This diagram has at its three corners (a) large clasts (>2 mm), (b) small clasts (0.1–2 mm) and matrix (<0.1 mm) and (c) crystalline cement. The 75% and 60% large-clast concentration limits provide a new quantitative calibration of this diagram, which Woodcock et al. (2006) could only indicate qualitatively. The 30% large-clast concentration line marks the transition proposed by Woodcock and Mort (in press) from fault breccia either to fault veins, if cement-rich, or to fine-grained fault rocks (mylonite, cataclasite or gouge, if dominated by fine clasts and matrix).

6. Conclusions

1. Breccias along the Dent Fault can be visually classified into crackle, mosaic or chaotic breccia, depending on the degree of clast disaggregation and misfit.
2. Image analysis of these breccias shows that the particle size distribution and its fractal dimension do not discriminate between the breccia classes. Clast sphericity and surface roughness show weak correlation with breccia class.
3. A better discriminant of breccia class is clast concentration. The Dent Fault breccias suggest that crackle breccia has at least 75% clasts, mosaic breccia 60–75% clasts and chaotic breccia less than 60% clasts.
4. The best discriminant is the average rotation of clasts away from a fully fitted texture, though this measurement cannot yet be fully automated. The analysed breccias suggest that crackle breccia involves average clasts rotation of less than 10°, mosaic breccia between 10° and 20°, and chaotic breccia more than 20°.
5. The quantification of breccia textures has allowed the construction of comparison charts for use in the field or laboratory.

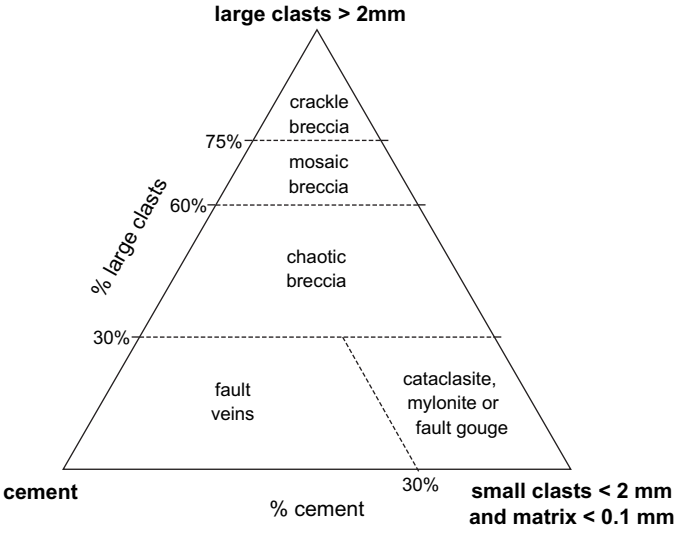

Fig. 8. The fault breccia classes as quantified in this paper plotted on the classification diagram of Woodcock et al. (2006) as amended by Woodcock and Mort (in press).

Acknowledgements

Our thanks go to Jon Tarasewicz, Jenny Omma and Niall Sayers for collecting the breccia samples and to David Cooke and Tom Blenkinsop for perceptive reviews of the manuscript.

References

Blenkinsop, T.G., 1991. Cataclasis and processes of particle size reduction. Pure and Applied Geophysics 136, 57–86.

Clark, C., James, P., 2003. Hydrothermal brecciation due to fluid pressure fluctuations: examples from the Olary Domain, South Australia. Tectonophysics 366, 187–206.

Coster, M., Chermant, J.L., 2001. Image analysis and mathematical morphology for civil engineering materials. Cement and Concrete Composites 23, 133–151.

Folk, R.L., 1965. Petrology of Sedimentary Rocks. Hemphill Publishing, Austin, Texas.

Higgins, M.W., 1971. Cataclastic rocks. In: Professional Paper, United States Geological Survey, 687, 97 p.

Jébrak, M., 1997. Hydrothermal breccias in vein-type ore deposits; a review of mechanisms, morphology and size distribution. Ore Geology Reviews 12, 111–134.

Killick, A.M., 2003. Fault rock classification: an aid to structural interpretation in mine and exploration geology. South African Journal of Geology 106, 395–402.

Koša, E., Hunt, D., Fitchen, W.M., Bockel-Rebelle, M.-O., Roberts, G., 2003. The heterogeneity of palaeocavern systems developed along syndepositional fault zones: the Upper Permian Capitan Platform, Guadalupe Mountains, U.S.A. In: Ahr, W.M., Harris, P.M., Morgan, W.A., Somerville, I.D. (Eds.), Permo-Carboniferous Carbonate Platforms and Reefs. Special Publication of the Society of Economic Paleontologists and Mineralogists, vol. 78, pp. 291–322.

Laznicka, P., 1988. Breccias and coarse fragmentites. Petrology, environments, associations, ores. Developments in Economic Geology 25.

Loucks, R.G., 1999. Paleocave carbonate reservoirs: origins, burial-depth modifications, spatial complexity, and reservoir implications. American Association of Petroleum Geologists Bulletin 83, 1795–1834.

Powers, M.C., 1953. A new roundness scale for sedimentary particles. Journal of Sedimentary Petrology 23, 117–119.

Rasband, W.S., 1997–2006. ImageJ. National Institutes of Health. Available from: http://rsb.info.nih.gov/ij/docs/.

Riley, N.A., 1941. Projection sphericity. Journal of Sedimentary Petrology 11, 94–95.

Sammis, C.G., Biegel, R.L., 1989. Fractals, fault gouge and friction. Pure and Applied Geophysics 131, 255–271.

Scion Corporation, 2006. Scion Image for Windows. Available from: http://www.scioncorp.com/pages/scion_image_windows.htm.

Sibson, R.H., 1977. Fault rocks and fault mechanisms. Journal of the Geological Society, London 133, 191–213.

Sibson, R.H., 1986. Brecciation processes in fault zones: inferences from earthquake rupturing. Pure and Applied Geophysics 124, 159–175.

Snoke, A.W., Tullis, J., Todd, V.R., 1998. Fault-related Rocks. Princeton University Press, Princeton.

Spry, A., 1969. Metamorphic Textures. Pergamon, London.

Tarasewicz, J.P.T., Woodcock, N.H., Dickson, J.A.D., 2005. Carbonate dilation breccias: examples from the damage zone to the Dent Fault, northwest England. Geological Society of America Bulletin 117, 736–745.

Taylor, R.G., 1992. Ore Textures, Recognition and Interpretation: Vol. 1, Infill. Economic Geology Research Unit, Townsville, Australia.

Turcotte, D.L., 1992. Fractals and Chaos in Geology and Geophysics. Cambridge University Press, Cambridge.

Waddell, H., 1933. Sphericity and roundness of rock particles. Journal of Geology 40, 443–451.

Woodcock, N.H., Mort, K. Classification of fault breccias and related fault rocks. Geological Magazine 145, in press.

Woodcock, N.H., Omma, J.E., Dickson, J.A.D., 2006. Chaotic breccia along the Dent Fault, NW England: implosion or collapse of a fault void? Journal of the Geological Society, London 163, 431–446.

Woodcock, N.H., Rickards, R.B., 2003. Transpressive duplex and flower structure: Dent Fault System, NW England. Journal of Structural Geology 25, 1981–1992.

Woodcock, N.H., Sayers, N.J., Dickson, J.A.D. Fluid flow history from damage zone cements near the Dent and Rawthey faults, NW England. Journal of the Geological Society, London 165, in press.